



Universiteit
Leiden

The Netherlands

Three-dimensional quantitative coronary angiography and the registration with intravascular ultrasound and optical coherence tomography

Tu, S.

Citation

Tu, S. (2012, February 28). *Three-dimensional quantitative coronary angiography and the registration with intravascular ultrasound and optical coherence tomography*. *ASCI dissertation series*. Retrieved from <https://hdl.handle.net/1887/18531>

Version: Corrected Publisher's Version

License: [Licence agreement concerning inclusion of doctoral thesis in the Institutional Repository of the University of Leiden](#)

Downloaded from: <https://hdl.handle.net/1887/18531>

Note: To cite this publication please use the final published version (if applicable).

CHAPTER

4

The Impact of Acquisition Angle Differences on Three-dimensional Quantitative Coronary Angiography

This chapter was adapted from:

The Impact of Acquisition Angle Differences on Three-dimensional
Quantitative Coronary Angiography
Shengxian Tu, Niels R. Holm, Gerhard Koning,
Michael Maeng, Johan H.C. Reiber
Catheterization and Cardiovascular Interventions. 2011,
Volume 78, Issue 2, Pages 214-222.

ABSTRACT

Background: Three-dimensional (3D) quantitative coronary angiography (QCA) requires two angiographic views to restore vessel dimensions. This study investigated the impact of acquisition angle differences (AAD) of the two angiographic views on the assessed dimensions by 3D QCA.

Methods: X-ray angiographic images of an assembled brass phantom with different types of straight lesions were recorded at multiple angiographic projections. The projections were randomly matched as pairs and 3D QCA was performed in those pairs with AAD larger than 25°. The lesion length and diameter stenosis in three different lesions, a circular concentric severe lesion (A), a circular concentric moderate lesion (B), and a circular eccentric moderate lesion (C), were measured by 3D QCA. The acquisition protocol was repeated for a silicone bifurcation phantom and the bifurcation angles and bifurcation core volume were measured by 3D QCA. The measurements were compared with the true dimensions if applicable and their correlation with AAD was studied.

Results: 50 matched pairs of angiographic views were analyzed for the brass phantom. The average value of AAD was $48.0 \pm 14.1^\circ$. The per cent diameter stenosis was slightly overestimated by 3D QCA for all lesions: A (error $1.2 \pm 0.9\%$, $p < 0.001$); B (error $0.6 \pm 0.5\%$, $p < 0.001$); C (error $1.1 \pm 0.6\%$, $p < 0.001$). The correlation of the measurements with AAD was only significant for lesion A ($R^2 = 0.151$, $p = 0.005$). The lesion length was slightly overestimated by 3D QCA for lesion A (error 0.06 ± 0.18 mm, $p = 0.026$), but well assessed for lesion B (error -0.00 ± 0.16 mm, $p = 0.950$) and lesion C (error -0.01 ± 0.18 mm, $p = 0.585$). The correlation of the measurements with AAD was not significant for any lesion. 40 matched pairs of angiographic views were analyzed for the bifurcation phantom. The average value of AAD was $49.1 \pm 15.4^\circ$. 3D QCA slightly overestimated the proximal angle (error $0.4 \pm 1.1^\circ$, $p = 0.046$) and the distal angle (error $1.5 \pm 1.3^\circ$, $p < 0.001$). The correlation with AAD was only significant for the distal angle ($R^2 = 0.256$, $p = 0.001$). The correlation of bifurcation core volume measurements with AAD was not significant ($p = 0.750$). Of the two aforementioned measurements with significant correlation with AAD, the errors tended to increase as AAD became larger.

Conclusions: 3D QCA can be used to reliably assess vessel dimensions and bifurcation angles. Increasing the acquisition angle difference of the two angiographic views does not increase accuracy and precision of 3D QCA for circular lesions or bifurcation dimensions.

4.1 INTRODUCTION

Over the past decades, the continuous developments in coronary visualization and quantitative systems have been motivated by the increasing need to better assess coronary atherosclerosis and by the on-line need for support of coronary interventions in cardiac catheterization laboratories. Recently developed three-dimensional quantitative coronary angiography (3D QCA) systems [1-5] aimed to combine two angiographic views from either biplane or monoplane angiograms to restore true vessel dimensions and hence, to resolve some of the well-known limitations of the conventional two-dimensional (2D) quantitative analysis [6-7], e.g., vessel foreshortening and out-of-plane magnification [8]. It has been shown that 3D QCA can better assess vessel segment length [2, 9] and bifurcation angles [10], as well as enabling the subsequent automated determination of optimal viewing angles for the subsequent stent deployment and positioning [11]. However, to the best knowledge of the authors, the impact of acquisition angle difference (AAD) of the two angiographic views on the 3D quantitative assessments has not been studied.

This study investigated the impact of AAD on the assessments of vessel dimensions including diameter stenosis, lesion length, bifurcation angles, and bifurcation core volume for phantoms with known dimensions.

4.2 MATERIALS AND METHODS

4.2.1 Assembled brass phantom

At the Leiden University Medical Center (Leiden, The Netherlands), X-ray images of an assembled brass phantom with different types of lesions was acquired by an X-ray angiogram (Infinix, Toshiba Medical Systems, Tokyo, Japan) at multiple viewing angles. Images were recorded at a resolution of 1024×1024 pixels and stored in DICOM (Digital Imaging and Communications in Medicine) format. The distance from the X-ray source to the image intensifier was set as 1000 mm for all acquisitions. For the entire acquisition procedure, the angulation angle (Cranial/ Caudal) of the C-arm was changed to 25 Caudal, 15 Caudal, 0°, 15 Cranial, and 25 Cranial, while the rotation angle (LAO/RAO) was changed to 45 LAO, 30 LAO, 15 LAO, 0°, 10 RAO, 20 RAO, 30 RAO, and 40 RAO. The angiographic image was recorded at each combination of rotation and angulation angles.

A total of 40 angiographic views with different acquisition angles were recorded. A computer program was used to randomly select each time two angiographic views with at least 25° in AAD and match the two views as a pair for the subsequent analysis. The AAD of the matched pair was defined

by the angle between the two central projection beams that were determined by the combination of rotation and angulation angles for each angiographic view, respectively. All analyses were performed by an experienced analyst using a recently developed 3D QCA software package (prototype version, Medis medical imaging systems by, Leiden, Netherlands) [2, 9, 11]. The software package excluded matched pairs that resulted in a perspective viewing angle (PVA) of less than 5° for the entire segment of interest. The PVA was defined as the angle between the epipolar line, being the projection of the X-ray beam directed towards a particular point on one of the projections onto the second projection, and the tangent of the vessel at the corresponding position [9]. Figure 4-1 shows an example of an excluded matched pair: The first angiographic view was acquired at 45 LAO, 25 Cranial and the second angiographic view at 45 LAO, 15 Caudal. In this case, the epipolar line was almost parallel to the vessel with an eccentric lesion at the corresponding marker position.

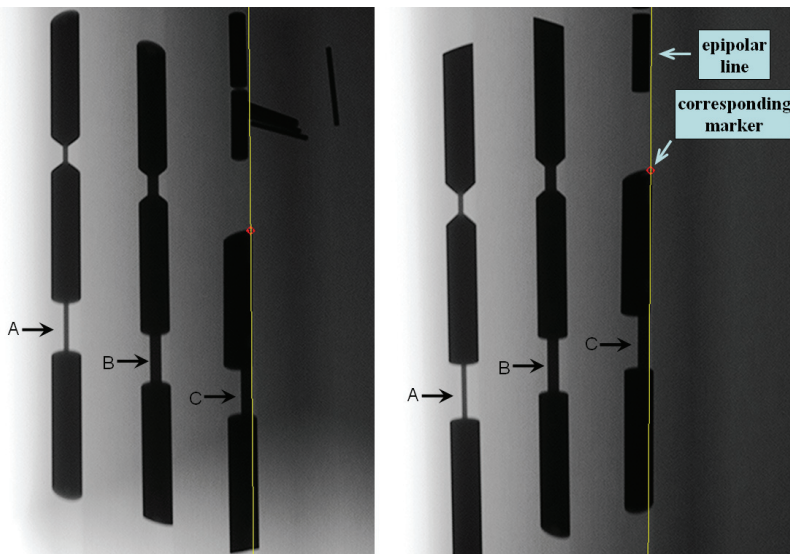


Figure 4-1. The excluded matched pair for 3D angiographic reconstruction. Left angiographic view at 45 LAO, 25 Cranial and right angiographic view at 45 LAO, 15 Caudal. The perspective viewing angle is almost zero for all three lesions. A is a circular concentric severe lesion; B is a circular concentric moderate lesion; and C is a circular eccentric moderate lesion.

For each included matched pair, the diameter stenosis and lesion length were assessed on 3 different types of straight lesions in the brass phantom, i.e., a circular concentric severe lesion (A), a circular concentric moderate lesion (B), and a circular eccentric moderate lesion (C). In addition, the reference diameter was also assessed on lesion B and

compared with the true dimension. Figure 4-1 shows the three types of lesions with known dimensions: A and B have circular concentric cross-sections with 80% and 60% diameter stenosis, respectively; C has circular eccentric cross-sections with 60% diameter stenosis; All three lesions have the same length (10.0 mm) and the same reference diameter (5.00 mm).

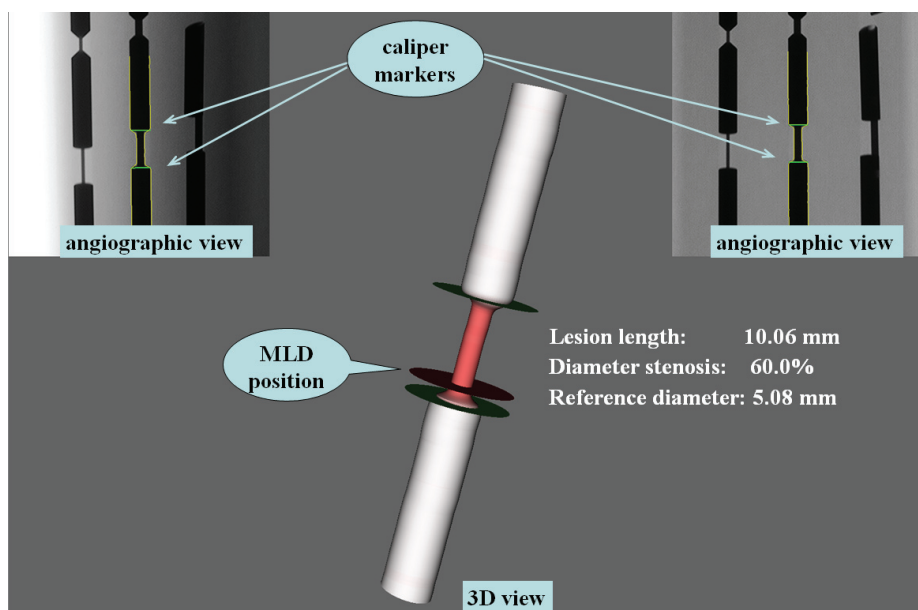


Figure 4-2. An analyzed matched pair of angiographic views and the 3D QCA assessed dimensions. Left angiographic view at 45 LAO, 15 Caudal and right angiographic view at 20 RAO, 15 Cranial. Diameter stenosis and reference diameter were reported at the MLD position.

Due to the angiographic isocenter offset introduced by gantry sag and other system distortions at different acquisition angles, one or two landmarks were used in the software package to correct the isocenter offset for each matched pair [9]. In the next step, lumen contours were detected automatically after specifying the proximal and distal positions for the segment of interest, followed by 3D reconstruction and quantifications. The position of the minimum lumen diameter (MLD) was automatically detected by the software package and diameter stenosis and the reference diameter were reported at that position. For lesion length assessment, the analyst moved the caliper markers to the lesion borders in one of the angiographic views, blinded to the measurement result. Since the repositioning of a marker in different views in the software package was supported by the fact that there existed a point correspondence between the 2D and 3D views, therefore, the caliper markers in the 3D view were synchronized to the lesion borders and the

3D lesion length was reported. Figure 4-2 shows an example of one analyzed matched pair and the 3D QCA assessed dimensions. In this case, the lesion has a length of 10.06 mm, diameter stenosis of 60.0%, and reference diameter of 5.08 mm.

The analyses on lesion B for the first 15 included matched pairs were repeated by the same analyst two months later, and by a second experienced analyst, both blinded to the earlier measurement results. From these measurements, intra- and inter-observer variabilities in the assessments of diameter stenosis, lesion length, and reference diameter were derived.

4.2.2 *Silicone bifurcation phantom*

At the Aarhus University Hospital, Skejby (Aarhus, Denmark), a silicone bifurcation phantom (Via Biomedical, CA, USA) with known dimensions was filled with iodinated contrast media (Visipaque 320, GE Healthcare, WI, USA) and scanned by an X-ray angiogram (AlluraXper, Philips Medical Systems, Best, The Netherlands). Images were recorded at a resolution of 1024×1024 pixels and stored in DICOM format. For the entire acquisition procedure, the angulation angle (Cranial/ Caudal) was changed to 20 Caudal, 0°, 20 Cranial, while the rotation angle (LAO/RAO) was changed to 45 LAO, 30 LAO, 15 LAO, 0°, 10 RAO, 20 RAO, 30 RAO, and 40 RAO. The angiographic image was recorded at each combination of rotation and angulation angles.

A total of 24 angiographic views with different acquisition angles were recorded. The same computer program was used to randomly select pairs of angiographic views with at least 25° in AAD. All analyses were performed by an experienced analyst using the same software package, blinded to the true bifurcation dimensions. For bifurcation analysis, the software package excluded those matched pairs that resulted in a PVA of less than 5° for either the entire main vessel or the entire sidebranch.

For each included matched pair, the bifurcation angles and bifurcation core volume were assessed. Two bifurcation angles, i.e., the proximal angle between the proximal main vessel (PMV) and the distal main vessel (DMV), and the distal angle between the DMV and the sidebranch (SB) [12], were measured. Figure 4-3 shows one angiographic view of an analyzed matched pair and the reconstructed bifurcation in 3D. In this case, the PVA was about 30° for the main vessel and 80° for the sidebranch. Hence, the matched pair was included for the subsequent analysis. The bifurcation core was separated by 3 delimiters: The proximal delimiter at the most distal position of PMV; The distal delimiter at the most proximal (carina) position of DMV; and the side delimiter at the most proximal (carina) position of SB. The cross-section of the bifurcation core

was of bean shape, as corresponded to the green contours that were superimposed onto the 3D bifurcation core in Figure 4-3. The size of the bifurcation core L was automatically determined by the combination of reference diameters of DMV and SB at the carina position. Therefore, the size of bifurcation core varied with the individual reconstructed bifurcation and more importantly, it was independent from the extent of lesion severity at the bifurcation core. Three directional vectors were estimated by applying linear regression algorithms on the sub-segments of PMV, DMV, and SB, respectively, with the same size of the bifurcation core. The proximal angle was defined by the angle between vector 1 and vector 3, while the distal angle was defined by vector 2 and vector 3. The bifurcation angles and bifurcation core volume were automatically calculated and reported by the software package. The true proximal and distal angles for the bifurcation phantom are 135° and 45° , respectively.

The analyses for the first 15 included matched pairs were repeated by the same analyst two months later, and by a second experienced analyst, both blinded to the earlier measurement results. From these measurements, intra- and inter-observer variabilities in the assessments of bifurcation angles and bifurcation core volume were derived.

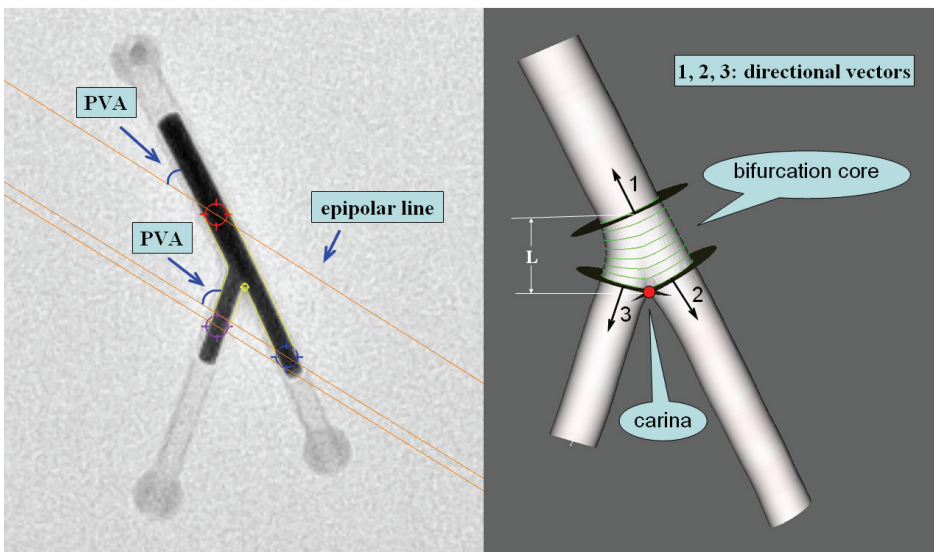


Figure 4-3. Angiographic view at 30° LAO, 20° Caudal of the silicone phantom and the reconstructed bifurcation in 3D. The 3D bifurcation core was separated by 3 delimiters (circular cross-sectional markers). The proximal angle was defined by the angle between vector 1 and vector 3, while the distal angle was defined by vector 2 and vector 3. The perspective viewing angle (PVA) was about 30° for the main vessel and 80° for the sidebranch.

4.3 STATISTICS

The results of 3D QCA measurements except for bifurcation core volume (unknown true dimension) were compared with the true dimensions by using paired *t*-test. The accuracy and precision were presented as measurement error and variability. Quantitative data were presented as mean difference \pm standard deviation and the correlations were assessed by using Pearson's correlation coefficient, providing the correlation coefficient (R^2). If the correlation was significant, the equation of the regression line was provided. A 2-sided *p*-value of <0.05 was considered to be significant. All statistical analyses were carried out by using a statistical software package (SPSS, version 16.0; SPSS Inc; Chicago, IL, USA).

4.4 RESULTS

A total of 52 matched pairs of angiographic views with AAD larger than 25° were generated for the brass phantom. Two matched pairs were excluded due to a small PVA for the entire vessel of interest. Therefore, 3D QCA was performed on the 50 remaining matched pairs. The values of AAD in the remaining matched pairs ranged from 27.1° to 85.5° , with an average value of $48.0 \pm 14.1^\circ$. The results of the 3D QCA assessments are given in Table I. In short, the per cent diameter stenosis was slightly overestimated by 3D QCA for all lesions: A (error $1.2 \pm 0.9\%$, $p < 0.001$); B (error $0.6 \pm 0.5\%$, $p < 0.001$); C (error $1.1 \pm 0.6\%$, $p < 0.001$). The intra- and inter-observer variabilities were 0.15 ± 0.54 and 0.33 ± 0.55 , respectively. The lesion length was slightly overestimated by 3D QCA for lesion A (error 0.06 ± 0.18 mm, $p = 0.026$), but well assessed for lesion B (error -0.00 ± 0.16 mm, $p = 0.950$) and lesion C (error -0.01 ± 0.18 mm, $p = 0.585$). The intra- and inter-observer variabilities were 0.08 ± 0.11 and 0.04 ± 0.14 , respectively. The reference diameter (only measured in lesion B) was slightly overestimated by 3D QCA (error 0.07 ± 0.03 mm, $p < 0.001$). The intra- and inter-observer variabilities were 0.01 ± 0.01 and 0.01 ± 0.01 , respectively. Figure 4-4 and 4-5 show the scatter plots of the errors in measuring the diameter stenosis and lesion length, respectively. The correlation of the diameter stenosis measurements with AAD was significant for lesion A ($R^2 = 0.151$, $p = 0.005$, linear regression equation: Error = $0.025 \times \text{AAD} - 0.019$), but not for lesion B ($R^2 = 0.012$, $p = 0.440$) and lesion C ($R^2 = 0.025$, $p = 0.275$). The measurement error for lesion A tended to increase as AAD became larger. The correlation of the lesion length measurements with AAD was not significant for any lesion: A ($R^2 = 0.002$, $p = 0.747$); B ($R^2 = 0.002$, $p = 0.772$); C ($R^2 = 0.000$, $p = 0.959$).

TABLE I. 3D QCA ASSESSMENTS FOR THE BRASS AND SILICON PHANTOMS

	Mean \pm SD	95% CI	Intra-observer error	Inter-observer error
Diameter stenosis (%)				
Lesion A	81.17 \pm 0.91	(80.92-81.43)	-	-
Lesion B	60.56 \pm 0.49	(60.42-60.70)	0.15 \pm 0.54	0.33 \pm 0.55
Lesion C	61.10 \pm 0.56	(60.94-61.26)	-	-
Lesion length (mm)				
Lesion A	10.06 \pm 0.18	(10.01-10.11)	-	-
Lesion B	10.00 \pm 0.16	(9.95-10.04)	0.08 \pm 0.11	0.04 \pm 0.14
Lesion C	9.99 \pm 0.18	(9.94-10.04)	-	-
Reference diameter (mm)	5.07 \pm 0.03	(5.06 - 5.08)	0.01 \pm 0.01	0.01 \pm 0.01
Proximal bifurcation angle ($^{\circ}$)	135.35 \pm 1.08	(135.01-135.70)	0.33 \pm 1.03	0.45 \pm 0.89
Distal bifurcation angle ($^{\circ}$)	46.54 \pm 1.32	(46.12-46.96)	0.84 \pm 1.02	0.26 \pm 0.78
Bifurcation core volume (mm ³)	29.51 \pm 1.11	(29.15-29.86)	0.13 \pm 1.55	0.01 \pm 0.90

CI, confidence interval

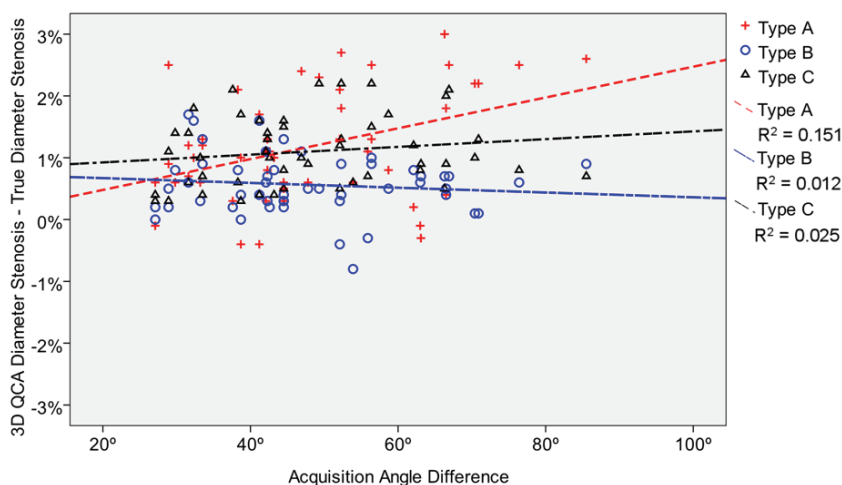


Figure 4-4. Diameter stenosis assessment by 3D QCA. The correlation of the 3D QCA measurements with AAD was significant for lesion A, but not for lesion B and lesion C.

A total of 45 matched pairs of angiographic views with AAD larger than 25° were generated for the silicone bifurcation phantom. Five matched pairs were excluded due to the small PVA for either the entire main vessel or the entire sidebranch. Therefore, 3D QCA was performed on 40 remaining matched pairs. The values of AAD in the remaining matched pairs ranged from 25.8° to 85.0° , with an average value of $49.1 \pm 15.4^{\circ}$. The results of the measurements are given in Table I. In short, 3D QCA slightly overestimated the proximal angle (error $0.4 \pm 1.1^{\circ}$, $p = 0.046$) and the distal angle (error $1.5 \pm 1.3^{\circ}$, $p < 0.001$). The intra- and inter-observer variabilities for the proximal angle were 0.33 ± 1.03 and 0.45 ± 0.89 , and for the distal angle were 0.84 ± 1.02 and 0.26 ± 0.78 ,

respectively. Figure 4-6 shows the scatter plot of the errors in measuring the bifurcation angles. The correlation with AAD was not significant for the proximal angle ($R^2 = 0.012, p = 0.502$), but significant for the distal angle ($R^2 = 0.256, p = 0.001$, linear regression equation: Error = $0.043 \times \text{AAD} - 0.590$). The measurement error for the distal angle tended to increase as AAD became larger. The bifurcation core had an average volume of $29.5 \pm 1.11 \text{ mm}^3$. The intra- and inter-observer variability was 0.13 ± 1.55 and 0.01 ± 0.90 , respectively. The correlation with AAD was not significant ($R^2 = 0.003, p = 0.750$).

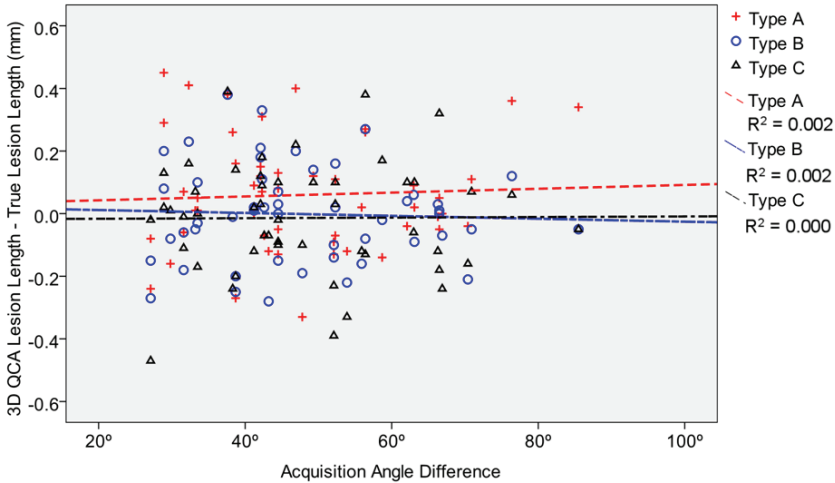


Figure 4-5. Lesion length assessment by 3D QCA. The correlation of the 3D QCA measurements with AAD was not significant for any lesion.

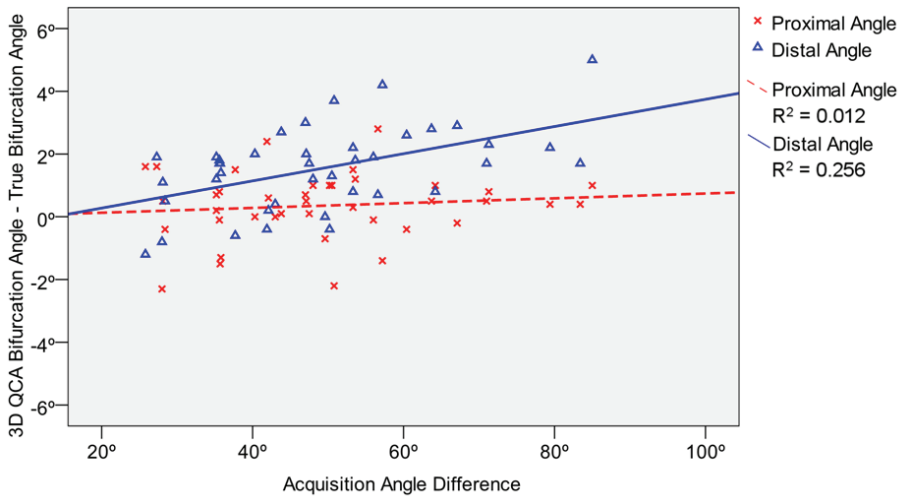


Figure 4-6. Bifurcation angle assessment by 3D QCA. The correlation of the 3D QCA measurements with AAD was significant for the distal angle, but not for the proximal angle.

4.5 DISCUSSIONS

Quantitative coronary angiography was first developed to quantify vessel motion and the effects of pharmacological agents on the regression and progression of coronary artery disease [13]. It has developed substantially over the past decades and has been applied worldwide for research and clinical purposes, in both off-line and on-line situations [7]. Although QCA techniques have been evolving with its wide applications [14-16], it remains as a limitation for 2D analysis that proper calibration, e.g., catheter calibration, needs to be performed for every analysis. If the vessel of interest is not in the calibration plane, the so-called out-of-plane magnification error will occur and hence, result in inaccurate measurements of absolute vessel dimensions. In addition, due to the 2D representation of the 3D vascular structures, the assessments of segment length and bifurcation angles depend to a great extent on vessel tortuosity and the angiographic viewing angle [11]. 3D QCA was motivated to overcome such limitations and to provide more support for coronary interventions in catheterization laboratories. By combining two angiographic views and the geometry of X-ray projections, 3D QCA was able to reconstruct vessel centerline and restore more details of the luminal cross-sections [1,9,18]. The continuous efforts in the DICOM standardization have made the automatic calibration procedure in 3D QCA feasible for most modern X-ray angiograms. Rapid improvements in computer hardware have also enabled real time 3D reconstruction on a conventional PC [2].

Despite the recent progresses, 3D QCA has been used in limited number of studies. One of the main reasons is the lack of standard operation procedures or protocols for performing 3D QCA. So far there is no official guideline for the angiographic acquisition dedicated for 3D QCA in a broad clinical setting. In general, the analyst selected two of the available angiographic views that were acquired during coronary angiography and used those two views for the subsequent 3D analysis. The optimal selection criteria remain unclear. Particularly, the impact of AAD of the two selected angiographic views on the 3D reconstruction and quantitative assessments has not been studied. This study showed that AAD did not have significant impact on 3D QCA for circular moderate lesions. For assessing bifurcation dimensions, the correlation between AAD and 3D QCA was only significant for the distal bifurcation angle. The correlation was weak and it indicated that the measurement error tended to increase as AAD became larger. One possible explanation is that as AAD increased, there were more overlaps between the DMV and the SB at their proximal parts. Therefore, the computer detected DMV centerline at

the proximal part could be slightly shifted toward the SB, resulting in an increase in the angle between the DMV and SB directional vectors, i.e., the distal angle.

Although this study showed that larger AAD did not increase accuracy and precision of 3D QCA in assessing circular lesions and bifurcation dimensions, non-circular lesions with asymmetric cross-sectional geometry are frequently encountered when assessing significant coronary stenoses in vivo [17]. Performing 3D QCA on two angiographic views with larger AAD may reveal more details of the luminal cross-sections and result in better luminal area assessment. However, larger AAD could potentially introduce more isocenter offset, as well as increasing the chance of vessel overlapping in the angiographic views and impair the assessments, especially for bifurcations where there tend to be more overlaps between the DMV and the SB as AAD increases. In other words, there are pros and cons of using larger AAD for assessing non-circular lesions in vivo and the optimal value may depend on individual vessel/bifurcation and the coronary anatomy. The actual impact of AAD on 3D QCA to assess lesions with asymmetric cross-sections still requires proper validations. It may be of interest to note that 3D QCA software packages generally calculate lesion length based on the approximated healthy vessel centerline, i.e., the so-call reference centerline, which calculates the length of the centerline in the vessel as if there is no obstruction [2]. Therefore, it is reasonable to expect that the impact of AAD on 3D QCA length assessment will be limited for vessels with non-circular lesions as well.

In this phantom study, the two angiographic views that were used for the 3D angiographic reconstruction were randomly selected by a computer program. As a result of this, 2 out of 52 matched pairs were excluded from the subsequent analyses for the brass phantom due to a small PVA (the angle between the epipolar line and the tangent of the vessel) for the entire vessel, while 5 out of 45 matched pairs were excluded for the silicone bifurcation phantom. When the PVA is 0° , there exist a huge number of feasible solutions which could satisfy the projection data. Figure 4-7 shows an example of different vessels that could generate the same lumen contours in the projection views, i.e., projection A and B. In this case, using projection A and B for the 3D angiographic reconstruction will result in a PVA of 0° for the entire vessel. In other words, the reconstruction of vessel centerline from projection A and B is not unique, since the PVA of the two projections is 0° for the entire vessel. In principle, the density information could be incorporated to decrease the feasible solutions; however, such solutions are hampered by the general quality of angiographic images in routine clinical practice, especially when

there are overlaps from other vessel segments. It implies that in practice using two angiographic views with larger PVA is preferred for 3D angiographic reconstruction and quantitative analysis. It is important to note that two angiographic views with larger AAD do not necessarily generate larger PVA, and vice versa. In theory, the PVA is determined by the tangent direction of the individual vessel and the geometry of the two angiographic views including acquisition angles and the distance from the X-ray source to the image intensifier. If one projection is already acquired, the practical approach to generate larger PVA for a specific vessel is to rotate the C-arm around the principal direction of the vessel to acquire the second projection. More specifically, the acquisition angle can be adjusted by changing the rotation angle (LAO/RAO) or the angulation angle (Cranial/Caudal) of the C-arm. If the first projection visualizes the lesion properly, and if the vessel of interest is positioned along the Cranial-Caudal direction, then changing the rotation angle to acquire the second projection will result in a large PVA. On the contrary, if the vessel of interest is positioned along the LAO-RAO direction, changing the angulation angle to acquire the second projection will result in a large PVA. For bifurcation cases, a trade-off between the main vessel and the sidebranch should be made so that both branches have relatively large PVA.

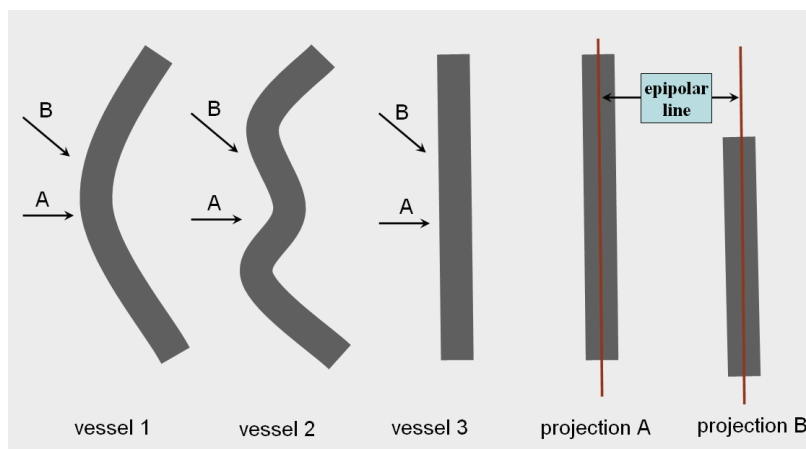


Figure 4-7. Different vessels that could generate the same lumen contours in the projections: Projection A and B have a perspective viewing angle (the angle between the epipolar line and the tangent of the vessel) of 0° for the entire vessel.

4.6 LIMITATIONS

Only lesions with circular concentric and circular eccentric cross-sections were investigated in this phantom study. The phantom studies do not account for the full complexity of angiographic acquisition artifacts in vivo, including angiographic system distortions, cardiac motions and

patient's respirations. In support of the findings, methods for the correction of such artifacts have been implemented in the software package.

4.7 CONCLUSIONS

3D QCA can be used to reliably assess vessel dimensions and bifurcation angles. Increasing the acquisition angle difference of the two angiographic views does not increase accuracy and precision of 3D QCA for circular lesions or bifurcation dimensions.

4.8 REFERENCES

1. Wahle A, Lopez JJ, Olszewski ME, et al. Plaque development, vessel curvature, and wall shear stress in coronary arteries assessed by X-ray angiography and intravascular ultrasound. *Medical Image Analysis* 2006; 10: 615–631.
2. Tu S, Huang Z, Koning G, et al. A novel three-dimensional quantitative coronary angiography system: In-vivo comparison with intravascular ultrasound for assessing arterial segment length. *Catheter Cardiovasc Interv* 2010; 76: 291–298.
3. Gollapudi RR, Valencia R, Lee SS, et al. Utility of three-dimensional reconstruction of coronary angiography to guide percutaneous coronary intervention. *Catheter Cardiovasc Interv* 2007; 69:479–482.
4. Rittger H, Schertel B, Schmidt M, et al. Three-dimensional reconstruction allows accurate quantification and length measurements of coronary artery stenoses. *EuroIntervention* 2009; 5:127–132.
5. Green NE, Chen SY, Hansgen AR, et al. Angiographic views used for percutaneous coronary interventions: a three-dimensional analysis of physician-determined vs. computer-generated views. *Catheter Cardiovasc Interv* 2005; 64: 451–459.
6. Reiber JHC, Serruys PW, Kooijman CJ, et al. Assessment of short-, medium-, and long-term variations in arterial dimensions from computer-assisted quantitation of coronary cineangiograms. *Circulation* 1985; 71: 280–288.
7. Reiber JHC, Tuinenburg JC, Koning G, et al. Quantitative coronary arteriography. In: *Coronary Radiology 2nd Revised Edition*, Oudkerk M, Reiser MF (Eds.), Series: *Medical Radiology, Sub series: Diagnostic Imaging*, Baert AL, Knauth M, Sartor K (Eds.). Springer-Verlag, Berlin-Heidelberg, 2009:41–65.
8. Koning G, Hekking E, Kempainen JS, et al. Suitability of the Cordis Stabilizer™ marker guide wire for quantitative coronary angiography calibration: An in vitro and in vivo study. *Catheter Cardiovasc Interv* 2001; 52: 334–341.
9. Tu S, Koning G, Jukema W, et al. Assessment of obstruction length and optimal viewing angle from biplane X-ray angiograms. *Int J Cardiovasc Imaging* 2010; 26: 5–17.
10. Girasis C, Serruys PW, Onuma Y, et al. 3-Dimensional Bifurcation Angle Analysis in Patients With Left Main Disease. *J Am Coll Cardiol Intv* 2010; 3: 41–48.
11. Tu S, Hao P, Koning G, et al. In-vivo assessment of optimal viewing angles from X-ray coronary angiography. *EuroIntervention* 2011; 7:112–120.
12. Louvard Y, Thomas M, Dzavik V, et al. Classification of coronary artery bifurcation lesions and treatments: time for a consensus! *Catheter Cardiovasc Interv* 2008; 71:175–83.

13. Brown BG, Bolson E, Frimer M, et al. Quantitative coronary angiography : estimation of dimensions, hemodynamic resistance, and atheroma mass of coronary artery lesions using arteriography in 256 nonoperated patients. *Circulation* 1977; 55: 329–337.
14. Janssen JP, Rares A, Tuinenburg JC, et al. New approaches for the assessment of vessel sizes in quantitative (cardio-) vascular X-ray analysis, *Int J Cardiovasc Imaging* 2010; 26: 259–271.
15. Lansky A, Tuinenburg J, Costa M, et al. Quantitative Angiographic Methods for Bifurcation Lesions: A Consensus Statement from the European Bifurcation Group. *Catheter Cardiovasc Interv* 2009; 73: 258–266.
16. Holm NR, Højdahl H, Lassen JF, et al, Quantitative coronary analysis in the Nordic Bifurcation studies, *Int J Cardiovasc Imaging* 2010; 27:175-180.
17. Arbab-Zadeh A, Texter J, Ostbye KM, et al. Quantification of lumen stenoses with known dimensions by conventional angiography and computed tomography: implications of using conventional angiography as gold standard. *Heart* 2010; 96: 1358-1363.
18. Tu S, Holm NR, Kong G, Huang Z, et al. Fusion of 3D QCA and IVUS/OCT. *Int J Cardiovasc imaging* 2011; 27:197–207.